Journal of Thermal Analysis and Calorimetry (2018) 133:1085–1092
https://doi.org/10.1007/s10973-018-7137-7

Sol–gel synthesis and thermal behavior of bioactive ferrous citrate–silica hybrid materials

Michelina Catauro[1] · Daniele Naviglio[2] · Roberta Risoluti[3] · Stefano Vecchio Ciprioti[4]

Received: 15 December 2017 / Accepted: 24 February 2018 / Published online: 6 March 2018

Abstract
Imbalance of the iron level in the body causes several diseases. In particular, the low level of iron, during pregnancy, is responsible for the iron deficiency anemia, and even of neurodegenerative diseases. Although the treatment of iron deficiency anemia with oral iron supplements has been known, this problem still afflicts many people. The aim of this work was the development of a system able to release ferrous ions in a controlled manner. Controlled drug release for medical applications, indeed, appears to be a very interesting alternative to a systemic therapy because it is assurance of treatment continuity and drug stability and optimizes drug absorption. For this purpose, ferrous citrate (Fe(II)C) was synthesized by a redox reaction between iron powder and citric acid. Fourier transform infrared spectroscopy (FTIR), 1,10-phenanthroline and sodium thiocyanate colorimetric assays confirmed that only Fe(II)C was obtained by redox reaction. Afterward, obtained Fe(II)C was embedded within a SiO_2 matrix in different mass percentage, by means of a sol–gel route. FTIR spectroscopy and simultaneous thermogravimetry/first-order derivative of thermogravimetry were used to confirm the Fe(II)C presence in the silica matrix and to investigate the thermal behavior of the sol–gel materials, respectively. The bioactivity test carried out by soaking the synthesized drug delivery systems in a simulated body fluid showed that the biological properties of the silica matrix are not modified by the presence of Fe(II)C.

Keywords Sol–gel method · Ferrous citrate · Thermal analysis · Drug delivery

Introduction

Iron is the transition element most abundant in the human body. It is involved in the process of the oxygen utilization, and it is the component of several oxidase and oxygenase enzymes. The level of iron in the body and its amount in the cells is strongly regulated to avoid its accumulation to a toxic level or its deficiency. Iron homeostasis regulation relies on cytoplasmic iron regulatory proteins, which modulate the translation and stability of ferritin and transferrin [1] and other enzymes involved in iron utilization, availability, uptake and release [2]. Dysfunctions in the homeostatic response to iron lead to an imbalance of the iron level, which can causes, in turn, several diseases. Iron overload and accumulation can generate oxidative stress by producing oxygen reactive species (ROS) that cause damage to membranes, proteins and DNA [3]. On the other hand, iron deficiency is considered to contribute as a risk factor to maternal and perinatal mortality and to the onset of disability, but also to contribute directly to the onset of cognitive impairment, neurodegenerative diseases, reduced work productivity and death due to severe anemia [4, 5]. For example, iron deficiency anemia is a risk factor of maternal mortality, causing the impairment of muscle function, which can lead to cardiac failure in childbirth [5]. Although it is known that the treatment of the diseases related to iron deficiency with iron supplements has beneficial effects (e.g., increase hemoglobin, serum ferritin, serum iron and transferrin saturation [4]), this problem still

✉ Michelina Catauro
michelina.catauro@unicampania.it

[1] Department of Engineering, University of Campania "Luigi Vanvitelli", Via Roma 29, 81031 Aversa, Italy

[2] Department of Chemical Sciences, University of Naples Federico II, Via Cintia, Naples, Italy

[3] Department of Chemistry, Sapienza University of Rome, P.le A.Moro 5, Rome, Italy

[4] Department S.B.A.I, Sapienza University of Rome, Via Del Castro Laurenziano 7, Rome, Italy

has a high effect and ranks number 9 among the 26 risk factors reported in the Global Burden of Disease 2000 project [6].

The need to develop a new strategy in the diseases therapy of iron deficiency, and in particular of the iron deficiency anemia, stimulates our research group to optimize systems able to release iron in a controlled manner. Controlled drug release for medical applications, indeed, is considered a very interesting alternative to systemic therapy because it assures treatment continuity and drug stability and optimizes drug absorption [7]. Therefore, the aim of this work was the development of therapeutic systems consisting of a SiO_2 matrix embedding different mass percentage of ferrous citrate (Fe(II)C) for drug delivery applications. Fe(II)C was synthesized by a redox reaction between iron powder and citric acid. The SiO_2 + Fe(II)C) hybrid materials were synthesized by sol–gel technique, a versatile method used to produce glasses, ceramics and organic/inorganic hybrid materials at low temperature [8, 9]. The process involves the transition of a system from a mostly colloidal liquid ('sol') into a solid 'gel.' The sol–gel method has many advantages, such as the purity of products and the possibility to incorporate thermolabile molecules [8]. Moreover, glasses and ceramics synthesized via sol–gel exhibit higher bioactivity and biocompatibility than those of materials with the same composition, but prepared using other techniques [10, 11]. Indeed, sol–gel-derived glasses have an inherent mesoporosity that gives them a larger surface area and potentially more rapid degradation rates than melt-derived glasses of similar composition [10, 11]. Moreover, the presence of –OH groups on their surface stimulates hydroxyapatite nucleation, promoting their easier osseointegration [10, 11]. Sol–gel glasses and ceramics have been proposed in many biomedical applications like artificial dental roots, as bone regenerative materials, coatings to improve biological performance of bioinert implants and drug delivery systems [12–15]. In particular, silica-based materials have shown positive biological properties [16–22], mainly ascribable to both their dissolution and degradation products (e.g., soluble silica) that are able to stimulate tissue growth [23]. On the other hand, Food and Drug Administration recognizes the use of Fe(II)C (see Fig. 1) in food as a nutrient supplement. Moreover, Yamashita et al. [24] showed that oral iron supplementation with a ferrous citrate salt (sodium ferrous citrate) decreases the risk of cardiovascular disease and death in iron-deficient maintenance hemodialysis (MHD) patients as well as ferric citrate. Iron deficiency, indeed, stimulates the transcription of the fibroblast growth factor 23 (FGF23), which is related to such diseases. This study proved that the release of Fe^{2+} increases the iron stores and reduced the serum level of FGF23 in iron-deficient MHD patients. Further, Zhao et al.

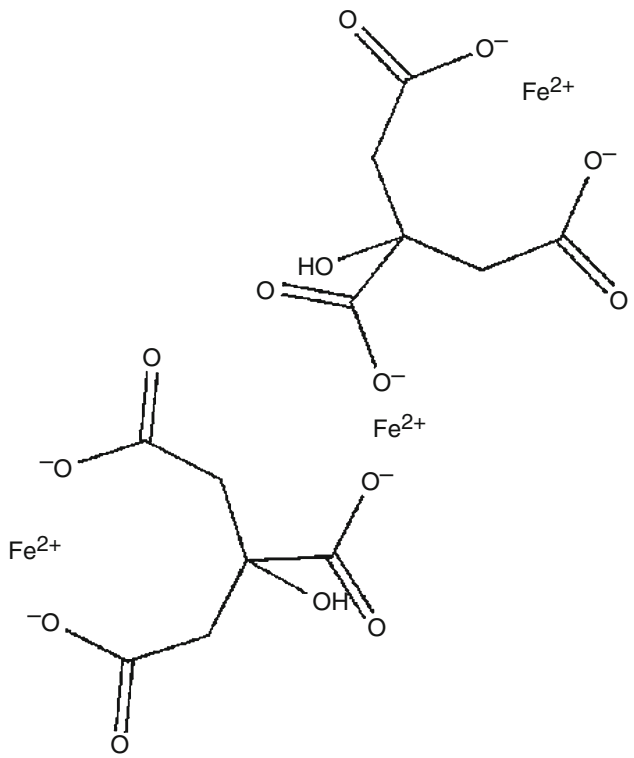

Fig. 1 Ferrous citrate structure

[25] reported that the treatment of renal ischemia with SFC associated with 5-aminolevulinic acid is useful to protect cardiomyocytes from hypoxia-induced apoptosis and, thus, to avoid the risk of cardiac disease associated to ischemia.

Fourier transform infrared (FTIR) spectroscopy and colorimetric assays were carried out to confirm that the redox reaction produced Fe(II)C and FTIR and simultaneous thermogravimetry/first-order derivative of thermogravimetry (TG/DTG) were used to characterize the materials and to investigate their thermal behavior. Furthermore, to confirm that the biological silica properties are retained in the synthesized SiO_2 + Fe(II)C hybrids, a bioactivity test was carried out. The materials were soaked in a simulated body fluid (SBF) and the ability to stimulate the hydroxyapatite nucleation was evaluated by FTIR and scanning electron microscopy (SEM) analysis.

Experimental

Ferrous citrate preparation

Ferrous citrate powder was synthesized according to the following redox reaction (Eq. (1)):

$$Fe(s) + C_6H_8O_7(s) \rightarrow FeC_6H_6O_7(s) + H_2(g) \quad (1)$$

between a fine iron powder (Sigma-Aldrich) and citric acid (> 99,5 Fluka, Buchs, Switzerland). The fine iron powder, with high reactive surface area, was added to a boiling aqueous solution (about 90 °C) of citric acid (in excess to allow the complete oxidation of iron). The reaction was carried out in a well-ventilated hood in order to remove the gaseous H_2 evolved during the process. A pearly white precipitate was obtained after 1 h, which was separated by vacuum filtration. The obtained powder was, then, washed with distilled water and dried in a glass desiccator. Qualitative colorimetric assays were carried out on the obtained precipitate fine powder, using 1,10-phenanthroline (Baker, Deventer, Holland) and sodium thiocyanate (Carlo Erba, Milano, Italy) in order to exclude the presence of Fe^{3+} and to confirm that it contains only Fe^{2+} ions. The first test allows detecting the presence of Fe^{2+} ions, whereas the second evaluates that of Fe^{3+} ions through the formation of colored complexes. In particular, 1,10-phenanthroline is able to form a red complex with Fe^{2+} ions, whereas Fe^{3+} ions form a blood-red complex with thiocyanate ions. 1,10-phenanthroline and sodium thiocyanate were solubilized in water purified using a milli-Q (Millipore, Bedford, MA, USA). Afterword, 50 mg of the precipitate was solubilized in 100 mL purified water. Then, 1 mL of both 1,10-phenanthroline and sodium thiocyanate solutions was added separately to two different aliquots of the so obtained yellow solution.

Sol–gel synthesis of the hybrid materials

The pure inorganic SiO_2 and the hybrids, consisting of the SiO_2 matrix in which 3, 5, 10, 15 and 20 mass% of ferrous citrate was embedded (SiO_2 + Fe(II)C), were synthesized by means of the sol–gel process. The inorganic silica gel was obtained by adding tetraethyl orthosilicate (TEOS; $Si(OC_2H_5)_4$; Sigma-Aldrich) to a solution of distilled water and 99.8% ethanol (EtOH, Sigma-Aldrich). Molar ratios equal to H_2O/TEOS = 23.5 and EtOH/TEOS = 6.2 were used in this study.

As far as the synthesis of the hybrid materials, different amount of Fe(II)C (prepared as described above) were dissolved in distilled water under stirring at 38 °C. To each obtained yellow solution, first 99.8% ethanol (Sigma-Aldrich) was added to make the solution more hydrophobic and second TEOS (insoluble in pure water). Figure 2 shows the flowchart of the sol–gel route. After gelation, the wet gels were dried in an oven at 50 °C for 24 h to remove the residual solvent.

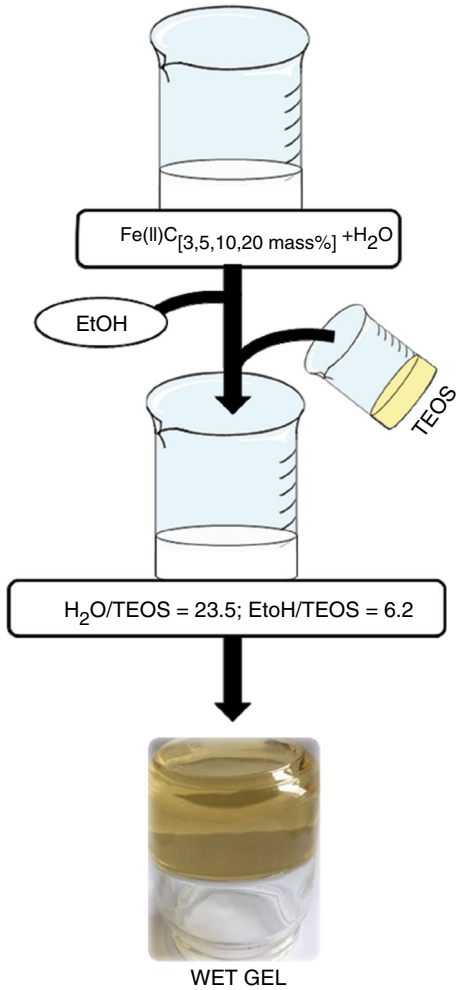

Fig. 2 Flowchart of the sol–gel synthesis

FTIR analysis of the Fe(II)C and of the hybrids

A Prestige 21 Shimadzu (Japan) FTIR instrument equipped with a deuterated tryglycine sulfate (with potassium bromide windows detector) was used to record Fourier transform infrared (FTIR) transmittance spectra of all samples in the 400–4000 cm^{-1} region, with resolution of 4 cm^{-1} (45 scans). KBr-pelletized disks containing 2 mg of each sample and 198 mg of KBr were made. The FTIR spectra were processed by Prestige software (IR solution).

Thermal analysis

TG/DTG curves were recorded using a Perkin-Elmer TGA7 Thermobalance (Massachusetts, USA) equipped with platinum crucibles. Approximately 3–5 mg of samples was heated in the temperature range 20–900 °C under a pure nitrogen atmosphere at a flow rate of 100 mL min^{-1}. All the experiments were conducted at 10 °C min^{-1} heating rate, as the best resolution rate.

Calibration of temperature was performed using the Curie-point transition of very pure standard metals or alloys (endpoint temperatures of Ni and alumel at 163 and 354 °C, in this study), as specified by the equipment recommendations. Diagnostics and acquisition of the TG data were carried out by Pyris software (Thermo Fisher Scientific Inc., Waltham, MA, USA) as ASCII files and processed by V-JDSU Unscrambler Lite (Camo software AS, Oslo, Norway).

Bioactivity test

The in vivo bioactivity test was carried out on synthesized hybrid materials by soaking the samples for 21 days in a simulated body fluid (SBF) solution. The dried gels were grinded in a mortar to obtain powders. A part of those powders was pressed by a hydraulic press (Specac, England) to obtain disks with diameter of 13 mm and thickness of 2 mm. Both the disks and the powders were soaked in SBF within polystyrene bottles and placed in a water bath at 37.0 ± 0.5 °C. The solution was replaced every 2 days to avoid depletion of the ionic species in the SBF due to the nucleation of biominerals on the samples. As the ratio between the total exposed surface and the volume solution influences the nucleation reaction, a constant ratio was chosen in agreement with the literature [26, 27]. After 21 days of exposure, both the disks and the powders were gently rinsed and dried in a glass desiccator. Afterward, the sample powders (2 mg) were mixed with KBr (198 mg), compressed to make tablets and subjected to FTIR analysis, whereas the surfaces of the disks were analyzed by using a scanning electron microscope (SEM Quanta 200, FEI, the Netherlands) equipped with energy-dispersive X-ray (EDX).

Results and discussion

Colorimetric assays

In the solution of Fe(II)C where 1,10-phenanthroline was added, a change of color from yellow to red is recorded. Two 1,10-phenanthroline bidentate ligand molecules can coordinate the ferrous ions in the citrate complex since they are already coordinated with two oxygen atoms of the citrate anions (see Fig. 3), whereas no color modification was observed in the second solution, where sodium thiocyanate was added. These findings confirm that the precipitate obtained by the redox reaction between iron powder and citric acid contains only Fe^{2+} ions.

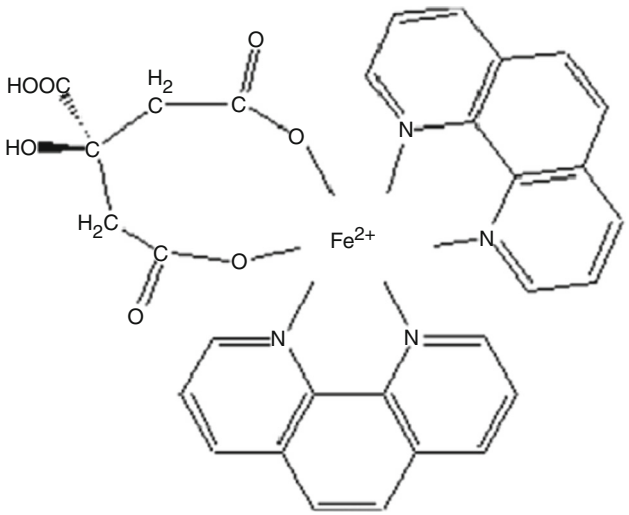

Fig. 3 Coordination of the 1,10-phenanthroline with ferrous citrate

FTIR analysis

Identification of the precipitate formed by the redox reaction between iron powder and citric acid (Eq. 1) as Fe(II)C, information on the structural organization of the synthesized materials and confirmation of the presence of Fe(II)C in the silica matrix were obtained by FTIR spectroscopy.

Figure 4 shows the spectra of pure SiO_2 (curve a) and Fe(II)C (curve g,) compared to the spectra of the SiO_2/Fe(II)C hybrids (curve from b to f). The FTIR spectrum of the precipitate (Fig. 4g) contains all the typical bands of the citrate salts [28–30]. FTIR results along with the

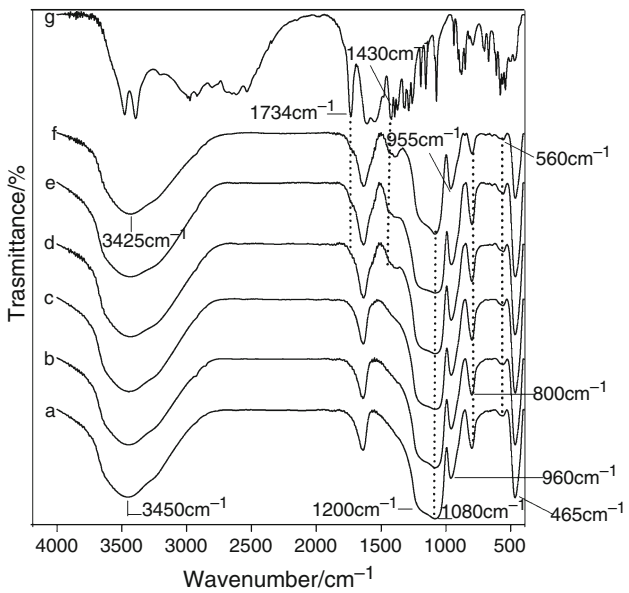

Fig. 4 FTIR spectra of (a) pure SiO_2, (b) SiO_2 + Fe(II)C 3 mass%, (c)SiO_2 + Fe(II)C 5 mass%, (d) SiO_2 + Fe(II)C 10 mass%, (e) SiO_2 + Fe(II)C 15 mass%, (f) SiO_2 + Fe(II)C 20 mass%, (g) pure Fe(II)C

colorimetric assays (described above) allow identifying it as Fe(II)C. Moreover, all the typical bands of the silica sol–gel materials [31–33] are visible in the FTIR spectra of the hybrids SiO_2/Fe(II)C (Fig. 4b–f), such as the strong band at 1080 cm^{-1} with a shoulder at 1200 cm^{-1}, as well as those at 800 and 465 cm^{-1} ascribable to asymmetric and symmetric Si–O–Si stretching and bending vibrations [34], respectively. The low-intensity band at 560 cm^{-1} was attributed to residual 4-membered siloxane rings in the silica network [31, 35–37]. Furthermore, the bands in the SiO_2/Fe(II)C spectra related to Si–OH bond vibrations [38] and O–H stretching [39] appear slightly shifted toward lower wavenumbers compared to those of pure SiO_2 (from 960 to 955 cm^{-1} and from 3450 to 3425 cm^{-1}, respectively). This result suggests the formation of interactions between Fe(II)C and the inorganic matrix. Furthermore, when a high amount of Fe(II)C is present in the material some bands related to citrate are visible as shoulder with respect to the silica signals. In particular, in the spectra of SiO_2 + Fe(II)C 10, 15 and 20 mass% (Fig. 4d-f) the weak signal at 1734 cm^{-1} due to the C=O stretching and the weak shoulders at 1550 and 1430 cm^{-1} ascribable to COO^- group are visible [28–30]. The weak intensity of the bands for Fe(II)C can be due to the overlap with the strong signals of the silica matrix.

Thermal analysis

The TG/DTG curves of both pure SiO_2 and Fe(II)C, as well as those of the hybrid materials SiO_2 + Fe(II)C (with 3–20 mass% of the latter), are shown in Fig. 5. As already shown in our recent studies [40, 41], pure SiO_2 undergoes dehydration up to 100 °C, followed by dehydroxylation, a slow release of water due to condensation of surface hydroxyl groups of the inorganic matrix up to 500 °C. Pure Fe(II)C losses only 1.1% of dehydration water up to 140 °C, and a remarkable three-step degradation takes place between 150 and 500 °C, being the first one associated to 50.5% of mass loss. The observed thermal behavior suggests that the Fe(II)C degradation follows a mechanism similar to that one reported for citric acid. According to [42], citric acid undergoes a dehydration process which leads to the formation of trans-aconitic acid. The least undergoes dehydration to trans-aconitic anhydride which, in turn, forms itaconic and citraconic anhydride by decarboxylation.

All the hybrid materials undergo dehydration up to 120 °C accompanied by mass losses between 17 and 22%, except for the rich-Fe(II)C material (containing 20 mass% of Fe(II)C) that loses more than 40% of hydration water. The higher loss of water is ascribable to the dehydration of the higher amount of Fe(II)C.

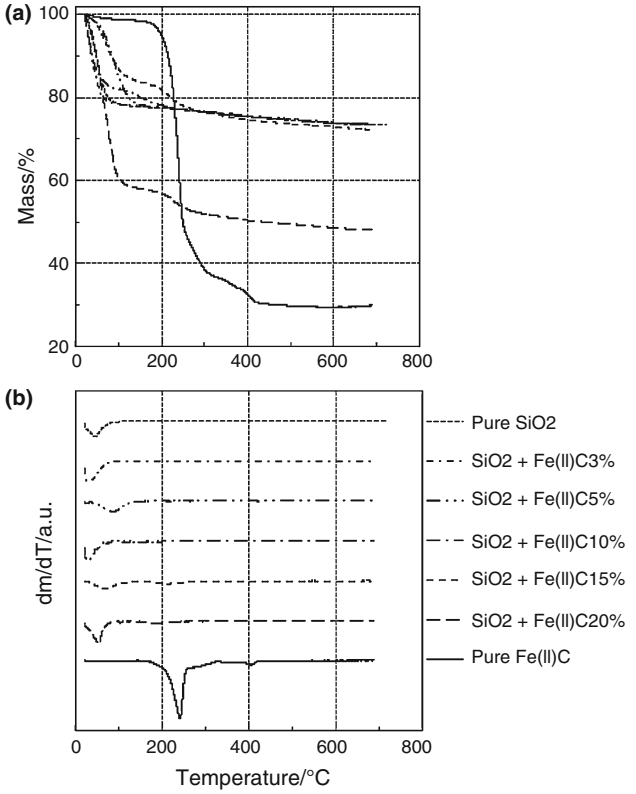

Fig. 5 TG/DTG curves (**a** and **b**, respectively) of: (—) pure SiO_2; (·-·-·) SiO_2 + Fe(II)C 3 mass%; (–··–) SiO_2 + Fe(II)C 5 mass%; (–·–) SiO_2 + Fe(II)C 10 mass%; (- - -) SiO_2 + Fe(II)C 15 mass%; (– –) SiO_2 + Fe(II)C 20 mass%; (—) pure Fe(II)C

Poor-Fe(II)C materials (with only 3 and 5% of Fe(II)C) seem to undergo only dehydroxylation similarly to what observed in the pure SiO_2 sample (Fig. 5). By contrast, the hybrids with 10–20 mass% of Fe(II)C undergo a second step of mass loss around 8–10%, probably ascribed to degradation of the organic component. This transformation takes place at lower temperature (100–280 °C) for the hybrid with 10 mass% of Fe(II)C (Fig. 5) and shifts toward higher temperatures (by 50 °C) for hybrids with 15 and 20 mass% of Fe(II)C. Unfortunately, the rate of mass loss for the process is not significant, and consequently, the corresponding DTG peaks are visible only for the last two samples.

This thermal degradation seems to end up to 400 °C for all hybrid materials and (in all cases) takes place at lower temperatures than in the pure Fe(II)C, concluding that the inorganic matrix can give a destabilizing effect to the organic component, favoring its degradation. This suggests that the incorporation of Fe^{2+} ions into the silica matrix occurs. The alkaline environment due to the presence of Fe(II)C in the water, indeed, can cause the dissociation of Si–OH groups and the release of H^+ which can be exchanged [26] with Fe^{2+} ions. Therefore, a free organic component more susceptible of thermal degradation could be produced.

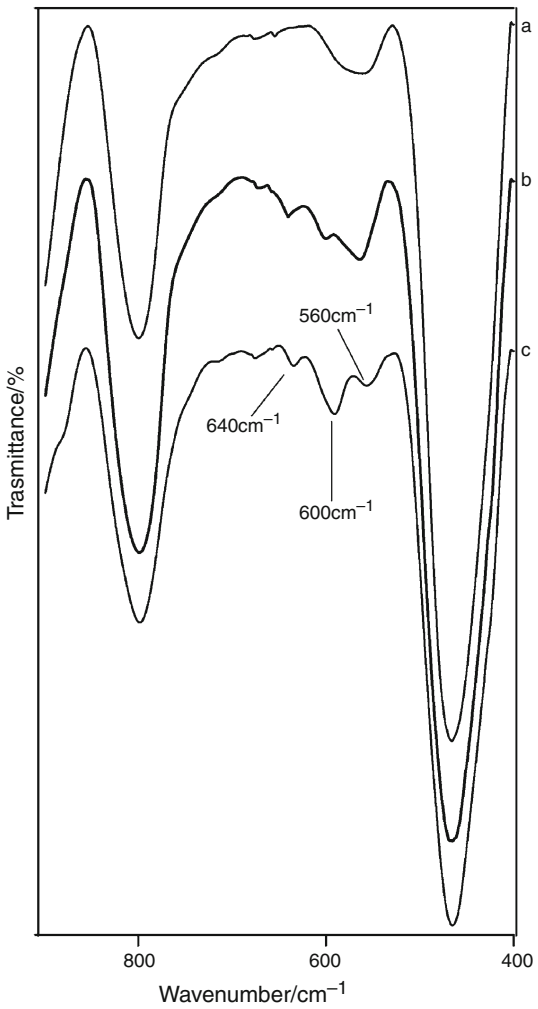

Fig. 6 FTIR spectra of **a** SiO_2 + Fe(II)C before and **b** SiO_2, **c** SiO_2 + Fe(II)C after 21 days of soaking in SBF

At temperatures higher than 400 °C, the hybrid materials slowly undergo a constant mass loss (1–2 mass% between 450 and 700 °C, reasonably ascribable to dehydroxylation.

Bioactivity test

A preliminary evaluation of hydroxyapatite formation in the materials' surface was carried out by FTIR analysis. Figure 6 shows the FTIR spectra of a representative SiO_2 + Fe(II)C hybrid recorded in the spectral region 900–400 cm^{-1} before soaking in SBF (Fig. 6a), compared to the spectra of pure SiO_2 (Fig. 6b) and representative SiO_2 + Fe(II)C hybrid (Fig. 6c) both after 21 days of exposure to the solution. In the spectra recorded after SBF exposure, the samples show a doublet signal at 600 cm^{-1} and 560 cm^{-1} and the band at 640 cm^{-1}, typical of the hydroxyapatite PO_4^{3-} groups [26].

The morphology and qualitative elemental analyses of the apatite deposition on the materials' surface after soaking in SBF were carried out by SEM/EDS microscopy (Fig. 7). The formation of crystals with the typical globular shape of the hydroxyl apatite was detected on the surface of all samples. EDS analysis confirmed that the globular precipitate consists of hydroxyapatite, as well as the ratio between the Ca and P atomic content equal to 1.6 [27]. Any significant difference in terms of the amount of precipitate apatite is recorded as function of the Fe(II)C content. Therefore, the results suggest that Fe(II)C content does not affect the bioactivity of the silica matrix.

Conclusions

In the present study, pure Fe(II)C powder was obtained by a redox reaction between a fine iron powder and citric acid. 1,10-phenanthroline and sodium thiocyanate quantitative colorimetric assays have proved that no Fe^{3+} but only Fe^{2+} ions are present in the obtained powder. Moreover, FTIR spectrum of the obtained powder shows all bands of citrate, leading to identify it as Fe(II)C. Different amounts of pure Fe(II)C obtained were incorporated in a silica matrix by a sol–gel process to obtain therapeutic systems to use in iron

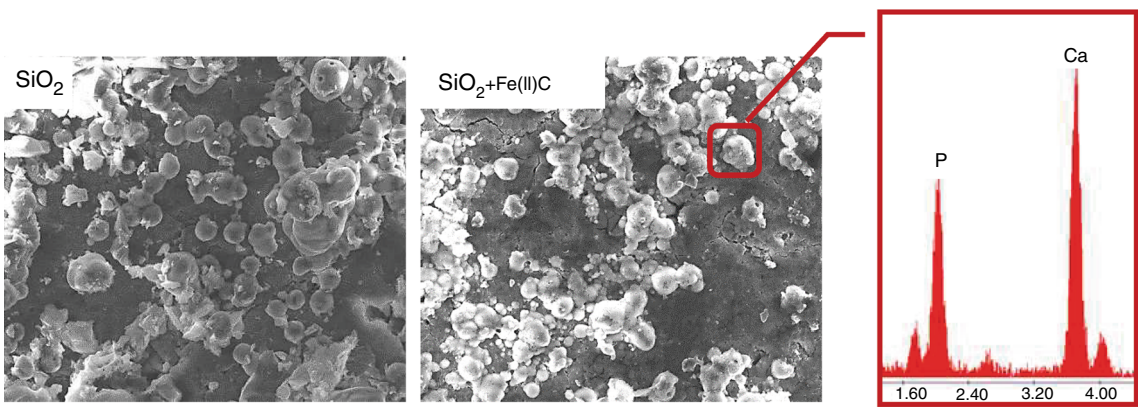

Fig. 7 SEM micrographs of **a** SiO_2 + Fe(II)C before and **b** SiO_2 + Fe(II)C after 21 days of soaking in SBF

deficiency anemia therapy. FTIR investigation proved that Fe(II)C is embedded in the matrix and interacts with it. The TG/DTG curves show that degradation of citrate anchored to the inorganic matrix takes place at lower temperatures, thus suggesting that the exchange of H^+ with Fe^{2+} ions occurs in the hybrids between silica and Fe(II)C.

On the other hand, bioactivity test proves that the presence of Fe(II)C does not affect the bioactivity of the silica matrix. Therefore, the obtained findings encourage the release kinetic study of Fe(II)C from SiO_2/Fe(II)C hybrids, in order to evaluate their potential use as drug delivery systems.

References

1. Cairo G, Recalcati S, Pietrangelo A, Minotti G. The iron regulatory proteins: targets and modulators of free radical reactions and oxidative damage1,2. Free Radic Biol Med. 2002;32(12):1237–43. https://doi.org/10.1016/S0891-5849(02)00825-0.
2. Cairo G, Pietrangelo A. Iron regulatory proteins in pathobiology. Biochem J. 2000;352(Pt 2):241–50.
3. Halliwell B, Gutteridge JM. Oxygen toxicity, oxygen radicals, transition metals and disease. Biochem J. 1984;219(1):1–14.
4. Allen LH. Anemia and iron deficiency: effects on pregnancy outcome. Am J Clin Nutr. 2000;71(5):1280s–4s.
5. Puntarulo S. Iron, oxidative stress and human health. Mol Asp Med. 2005;26(4):299–312. https://doi.org/10.1016/j.mam.2005.07.001.
6. Stoltzfus RJ. Iron deficiency: global prevalence and consequences. Food Nutr Bull. 2003;24(4_suppl2):S99–103. https://doi.org/10.1177/15648265030244s206.
7. Somayaji BV, Jariwala U, Jayachandran P, Vidyalakshmi K, Dudhani RV. Evaluation of antimicrobial efficacy and release pattern of tetracycline and metronidazole using a local delivery system. J Periodontol. 1998;69(4):409–13. https://doi.org/10.1902/jop.1998.69.4.409.
8. Brinker C, Scherer G. Sol-gel science: the physics and chemistry of sol-gel processing. San Diego: Academic press; 1989.
9. Catauro M, Pagliuca C, Lisi L, Ruoppolo G. Synthesis of alkoxide-derived V-Nb catalysts prepared by sol-gel route. Thermochim Acta. 2002;381(1):65–72. https://doi.org/10.1016/s0040-6031(01)00646-3.
10. Gupta R, Kumar A. Bioactive materials for biomedical applications using sol-gel technology. Biomed Mater. 2008;3(3):034005.
11. Martin RA, Yue S, Hanna JV, Lee PD, Newport RJ, Smith ME, et al. Characterizing the hierarchical structures of bioactive sol-gel silicate glass and hybrid scaffolds for bone regeneration. Philos Trans R Soc A Math Phys Eng Sci. 1963;2012(370):1422–43. https://doi.org/10.1098/rsta.2011.0308.
12. Vallet-Regí M. Ceramics for medical applications. J Chem Soc Dalton Trans. 2001;2:97–108.
13. Catauro M, Bollino F, Papale F. Biocompatibility improvement of titanium implants by coating with hybrid materials synthesized by sol-gel technique. J Biomed Mater Res Part A. 2014;102(12):4473–9. https://doi.org/10.1002/jbm.a.35116.
14. Catauro M, Bollino F, Papale F, Pacifico S, Galasso S, Ferrara C, et al. Synthesis of zirconia/polyethylene glycol hybrid materials by sol-gel processing and connections between structure and release kinetic of indomethacin. Drug Deliv. 2014;21(8):595–604. https://doi.org/10.3109/10717544.2013.865816.
15. Bollino F, Armenia E, Tranquillo E. Zirconia/hydroxyapatite composites synthesized via sol-gel: Influence of hydroxyapatite content and heating on their biological properties. Materials. 2017. https://doi.org/10.3390/ma10070757.
16. Catauro M, Bollino F, Papale F, Piccolella S, Pacifico S. Sol-gel synthesis and characterization of SiO_2/PCL hybrid materials containing quercetin as new materials for antioxidant implants. Mater Sci Eng C. 2016;58:945–52. https://doi.org/10.1016/j.msec.2015.09.054.
17. Vallet-Regi M, Balas F. Silica materials for medical applications. Open Biomed Eng J. 2008;2:1–9. https://doi.org/10.2174/1874120700802010001.
18. Catauro M, Bollino F, Papale F, Vecchio Ciprioti S. Investigation on bioactivity, biocompatibility, thermal behavior and antibacterial properties of calcium silicate glass coatings containing Ag. J Non-Cryst Solids. 2015;422:16–22. https://doi.org/10.1016/j.jnoncrysol.2015.04.037.
19. Catauro M, Laudisio G, Costantini A, Fresa R, Branda F. Low temperature synthesis, structure and bioactivity of 2CaO·3SiO2 glass. J Sol-Gel Sci Technol. 1997;10(2):231–7.
20. Catauro M, Bollino F, Papale F, Gallicchio M, Pacifico S. Synthesis and chemical characterization of new silica polyethylene glycol hybrid nanocomposite materials for controlled drug delivery. J Drug Deliv Sci Technol. 2014;24(4):320–5. https://doi.org/10.1016/s1773-2247(14)50069-x.
21. Blanco I. Polyhedral oligomeric silsesquioxanes (POSS)s in medicine. J Nanomed. 2018;1(1):1002.
22. Russo V, Tesser R, Trifuoggi M, Giugni M, Di Serio M. A dynamic intraparticle model for fluid–solid adsorption kinetics. Comput Chem Eng. 2015;74:66–74. https://doi.org/10.1016/j.compchemeng.2015.01.001.
23. Midha S, Kim TB, van den Bergh W, Lee PD, Jones JR, Mitchell CA. Preconditioned 70S30C bioactive glass foams promote osteogenesis in vivo. Acta Biomater. 2013;9(11):9169–82. https://doi.org/10.1016/j.actbio.2013.07.014.
24. Yamashita K, Mizuiri S, Nishizawa Y, Kenichiro S, Doi S, Masaki T. Oral iron supplementation with sodium ferrous citrate reduces the serum intact and c-terminal fibroblast growth factor 23 levels of maintenance haemodialysis patients. Nephrology. 2017;22(12):947–53. https://doi.org/10.1111/nep.12909.
25. Zhao M, Zhu P, Fujino M, Nishio Y, Chen J, Ito H, et al. 5-Aminolevulinic acid with sodium ferrous citrate induces autophagy and protects cardiomyocytes from hypoxia-induced cellular injury through MAPK-Nrf-2-HO-1 signaling cascade. Biochem Biophys Res Commun. 2016;479(4):663–9. https://doi.org/10.1016/j.bbrc.2016.09.156.
26. Catauro M, Bollino F, Renella RA, Papale F. Sol–gel synthesis of SiO_2–CaO–P_2O_5 glasses: influence of the heat treatment on their bioactivity and biocompatibility. Ceram Int. 2015;41(10, Part A):12578–88. https://doi.org/10.1016/j.ceramint.2015.06.075.
27. Kokubo T, Takadama H. How useful is SBF in predicting in vivo bone bioactivity? Biomaterials. 2006;27(15):2907–15. https://doi.org/10.1016/j.biomaterials.2006.01.017.
28. Bichara LC, Lanús HE, Ferrer EG, et al. Vibrational study and force field of the citric acid dimer based on the SQM methodology. Adv Phys Chem. 2011. https://doi.org/10.1155/2011/347072.
29. Coates J. Interpretation of infrared spectra, a practical approach. encyclopedia of analytical chemistry. Hoboken: Wiley; 2006.
30. Tsimbler SM, Shevchenko LL, Grigor'eva VV. The IR absorption spectra of the tartrate and citrate complexes of nickel, cobalt, and iron. J Appl Spectrosc. 1969;11(3):1096–101. https://doi.org/10.1007/bf00607851.

31. Adeogun MJ, Hay JN. Structure control in sol-gel silica synthesis using ionene polymers. 2: evidence from spectroscopic analysis. J Sol-Gel Sci Technol. 2001;20:119–28.
32. Innocenzi P. Infrared spectroscopy of sol-gel derived silica-based films: a spectra-microstructure overview. J Non-Cryst Solids. 2003;316:309–19. https://doi.org/10.1016/s0022-3093(02)01637-x.
33. Catauro M, Bollino F, Mozzati MC, Ferrara C, Mustarelli P. Structure and magnetic properties of SiO2/PCL novel sol-gel organic-inorganic hybrid materials. J Solid State Chem. 2013;203:92–9. https://doi.org/10.1016/j.jssc.2013.04.014.
34. Blanco I, Bottino FA, Abate L. Influence of n-alkyl substituents on the thermal behaviour of polyhedral oligomeric silsesquioxanes (POSSs) with different cage's periphery. Thermochim Acta. 2016;623:50–7. https://doi.org/10.1016/j.tca.2015.11.013.
35. Nedelec JM, Hench LL. Ab initio molecular orbital calculations on silica rings. J Non-Cryst Solids. 1999;255:163–70. https://doi.org/10.1016/s0022-3093(99)00367-1.
36. Yoshino H, Kamiya K, Nasu H. IR study on the structural evolution of sol-gel-derived silica gels in the early stage of conversion to glasses. J Non-Cryst Solids. 1990;126:68–78. https://doi.org/10.1016/0022-3093(90)91024-l.
37. Chen Y-C, Liu C-P, Yang C-K, Huang B-Y, Liu C-Y. Preparation and release properties of sol-gel encapsulated proteins. J Anal Sci Methods Instrum. 2013;3:11–6. https://doi.org/10.4236/jasmi.2013.33a002.
38. Simon V, Eniu D, Gritco A, Simon S. Thermal and spectroscopic investigation of sol-gel derived aluminosilicate bioglass matrices. J Optoelectron Adv Mater. 2007;9:3368–71.
39. Georgieva I, Danchova N, Gutzov S, Trendafilova N. DFT modeling, UV-Vis and IR spectroscopic study of acetylacetone-modified zirconia sol-gel materials. J Mol Model. 2012;18:2409–22. https://doi.org/10.1007/s00894-011-1257-3.
40. Vecchio Ciprioti S, Catauro M. Synthesis, structural and thermal behavior study of four Ca-containing silicate gel-glasses: activation energies of their dehydration and dehydroxylation processes. J Therm Anal Calorim. 2016;123(3):2091–101. https://doi.org/10.1007/s10973-015-4729-3.
41. Vecchio Ciprioti S, Catauro M, Bollino F, Tuffi R. Thermal behavior and dehydration kinetic study of SiO2/PEG hybrid gel glasses. Polym Eng Sci. 2017;57(6):606–12. https://doi.org/10.1002/pen.24561.
42. Wyrzykowski D, Hebanowska E, Nowak-Wiczk G, Makowski M, Chmurzyński L. Thermal behaviour of citric acid and isomeric aconitic acids. J Therm Anal Calorim. 2011;104(2):731–5. https://doi.org/10.1007/s10973-010-1015-2.